Disorder-induced broadening of the density of states for two-dimensional electrons with strong spin-orbit coupling

A. G. Galstyan and M. E. Raikh
Department of Physics, University of Utah, Salt Lake City, Utah 84112
(Received 10 February 1998; revised manuscript received 4 May 1998)

We theoretically study the disorder-induced smearing of the density of states in a two-dimensional electron system, taking into account a spin-orbit term in the Hamiltonian of a free electron. We show that the characteristic energy scale for the smearing increases with increasing spin-orbit coupling. We also demonstrate that in the limit of a strong spin-orbit coupling the diagrams with self-intersections make a parametrically small contribution to the self-energy. As a result, the coherent potential approximation becomes asymptotically exact in this limit. The tail of the density of states has an energy scale which is much smaller than the magnitude of the smearing. We find the shape of the tail using the instanton approach. [S0163-1829(98)05836-6]

It is well known how the random potential smears the band-edge in a two-dimensional (2D) system. In the case of a white-noise potential with a correlator $\overline{V(\mathbf{r})V(\mathbf{r}')}=\gamma\delta(\mathbf{r}-\mathbf{r}')$, the characteristic energy scale for the smearing can be estimated as $E_{2D}=\gamma m/\hbar^2$. Deep in the tail ($E<0$, $|E|\gg E_{2D}$) the density of states (DOS) falls off exponentially

$$\rho(E)\propto\exp\left(-\xi\frac{|E|}{E_{2D}}\right), \tag{1}$$

where the numerical factor ξ is approximately $\xi\approx 5.8$.[1,2] The form of tail (3) follows from the instanton approach developed in Refs. 3 and 4 (see also Refs. 5 and 6). The prefactor in Eq. (1), including the numerical coefficient, was derived in Ref. 2. In the intermediate region, $E\sim E_{2D}$, the exact form of the DOS is unknown. Within the coherent potential approximation it was studied in Ref. 1. The autors of Ref. 1 have also performed the approximate matching of the coherent potential result and tail (1).

Spin-orbit (SO) interaction modifies the energy spectrum of 2D electrons. The origin of this modification is either the absence of inversion symmetry in the bulk[7,8] or the asymmetry of the confinement potential. In the latter case the SO interaction can be taken into account by adding to the Hamiltonian of a free electron the term[9]

$$\hat{H}_{SO}=\alpha(\hat{\boldsymbol{\sigma}}\times\mathbf{k})\cdot\mathbf{n}, \tag{2}$$

where the components of $\hat{\boldsymbol{\sigma}}$ are the Pauli matrices, $\mathbf{n}\|\mathbf{z}$ is the normal to the 2D plane, α is the SO coupling constant, and $\mathbf{k}$ stands for the electron wave vector. The energy spectrum of the Hamiltonian

$$\hat{H}=\frac{\hbar^2}{2m}k^2+\hat{H}_{SO}=\begin{pmatrix}\frac{\hbar^2}{2m}k^2 & \alpha(k_x+ik_y)\\ \alpha(k_x-ik_y) & \frac{\hbar^2}{2m}k^2\end{pmatrix} \tag{3}$$

consists of two branches

$$E_{1,2}(\mathbf{k})=\frac{\hbar^2k^2}{2m}\mp\alpha|\mathbf{k}|. \tag{4}$$

The corresponding eigenstates have the form

$$\Psi^{(1,2)}_{\mathbf{k}}(\mathbf{r})=e^{i\mathbf{kr}}\chi^{(1,2)}_{\mathbf{k}}, \tag{5}$$

where the spinors $\chi^{(1,2)}_{\mathbf{k}}$ are defined as

$$\chi^{(1)}_{\mathbf{k}}=\frac{1}{\sqrt{2}}\begin{pmatrix}e^{i\phi_{\mathbf{k}}}\\ -1\end{pmatrix},\quad \chi^{(2)}_{\mathbf{k}}=\frac{1}{\sqrt{2}}\begin{pmatrix}1\\ e^{-i\phi_{\mathbf{k}}}\end{pmatrix}. \tag{6}$$

Here $\phi_{\mathbf{k}}$ is the azimuthal angle of the wave vector $\mathbf{k}$. The lower branch $E_1(\mathbf{k})$ has a minimum at $k=k_0=\alpha m/\hbar^2$ with a depth $\Delta=m\alpha^2/2\hbar^2$. In the absence of a disorder the densities of states corresponding to each branch have the form

$$\rho^{(0)}_{1,2}(E)=\frac{m}{2\pi\hbar^2}\frac{\sqrt{1+E/\Delta}\pm 1}{\sqrt{1+E/\Delta}}. \tag{7}$$

It is seen that $\rho^{(0)}_1(E)$ is 1D like, in the sense that it diverges as $(-|E|+\Delta)^{-1/2}$. The energy spectrum (4) and the densities of states (7) are shown in Fig. 1.

The relation between the disorder and the SO coupling is measured by a dimensionless parameter

$$\kappa=\frac{E_{2D}}{2\Delta}=\frac{\gamma}{\alpha^2}. \tag{8}$$

It is clear that, if $\kappa\gg 1$, then the spin-orbit term has a negligible effect on the DOS. In other words, in the limit of weak SO coupling the smearing is still determined by the energy scale E_{2D}. In the present paper we study the opposite limit of a strong SO coupling (or weak disorder), $\kappa\ll 1$. Remarkably, in this case the DOS can be found *exactly*.

Let us first determine the characteristic energy scale E_{1D} for disorder-induced broadening.[10] Using the golden rule, the relaxation time for an electron with energy close to $E=-\Delta$ can be written as $\hbar/\tau_E\sim\gamma\rho^{(0)}_1(E)$. Then E_{1D} can be found from the condition $E_{1D}\sim\hbar/\tau_{E_{1D}}$, yielding

$$E_{1D}=\frac{m}{\hbar^2}(\gamma\alpha)^{2/3}. \tag{9}$$

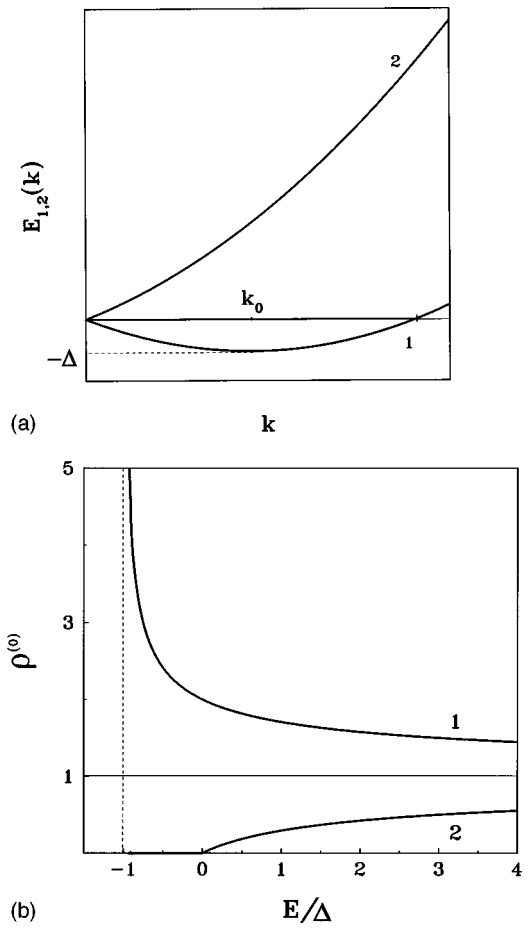

FIG. 1. (a) The energy spectrum of a 2D system with spin-orbit coupling. (b) The density of states for two branches of the spectrum.

We see that for $\kappa \ll 1$ the energy scale is much larger than E_{2D} but much smaller than the depth of the minimum:

$$E_{1D} = \frac{E_{2D}}{\kappa^{2/3}} = \kappa^{1/3}\Delta. \tag{10}$$

This last condition allows a strong simplification in the calculation of the DOS. Indeed, Eq. (10) suggests that the states in the region of smearing are composed of plane waves with magnitudes of wave vectors close to k_0,

$$|\mathbf{k}| - k_0 \sim \sqrt{2mE_{1D}/\hbar^2} \sim \kappa k_0 \ll k_0. \tag{11}$$

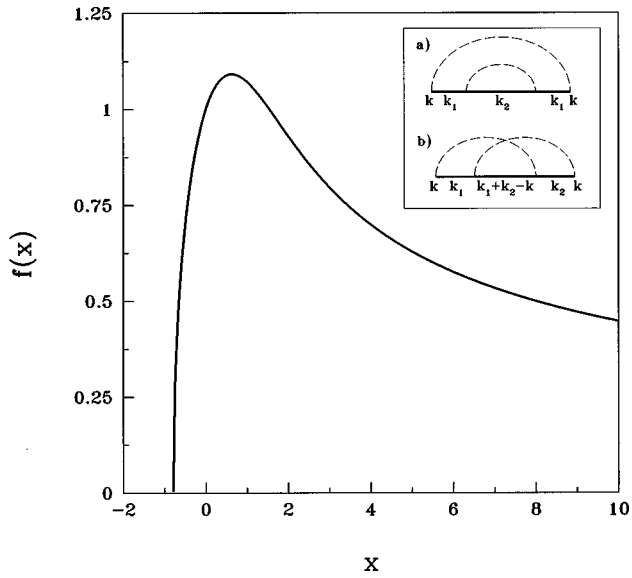

FIG. 2. Dimensionless function $f(x)$ defined by Eq. (24). Inset: two second-order diagrams for the self-energy Σ. (a) The diagram without self-intersection. (b) The diagram with self-intersection.

If we rewrite the energy spectrum $E_1(\mathbf{k})$ as

$$E_1(\mathbf{k}) = -\Delta + \frac{\hbar^2}{2m}(|\mathbf{k}| - k_0)^2, \tag{12}$$

then Eq. (11) allows to consider the second term as a small correction. The crucial observation, which allows the calculation of the DOS

$$\rho(E) = \frac{1}{\pi}\mathrm{Im}\sum_k \frac{|\chi_{\mathbf{k}}^{(1)}|^2}{E - E_1(\mathbf{k}) - \Sigma_{\mathbf{k}}(E)} \tag{13}$$

in the closed form, is that under the condition $\kappa \ll 1$ the contribution of the diagrams with self-intersections to the self-energy, $\Sigma_{\mathbf{k}}(E)$, is much smaller than the contribution of diagrams without self-intersections. In other words, in the strong SO coupling limit the coherent potential approximation *becomes asymptotically exact*. To illustrate this statement, consider two second-order diagrams for the self-energy shown in inset of Fig. 2. The contributions of the diagrams (a) and (b) to Im Σ are

$$\mathrm{Im}\,\Sigma^{(1)} = \gamma^2 \mathrm{Im}\int \frac{d^2\mathbf{k}_1}{(2\pi)^2}\int \frac{d^2\mathbf{k}_2}{(2\pi)^2}\frac{|(\chi_{\mathbf{k}}^{*(1)}\chi_{\mathbf{k}_1}^{(1)})(\chi_{\mathbf{k}_1}^{*(1)}\chi_{\mathbf{k}_2}^{(1)})|^2}{[E - E_1(\mathbf{k}_1)]^2[E - E_1(\mathbf{k}_2)]}, \tag{14}$$

$$\mathrm{Im}\,\Sigma^{(2)} = \gamma^2 \mathrm{Im}\int \frac{d^2\mathbf{k}_1}{(2\pi)^2}\int \frac{d^2\mathbf{k}_2}{(2\pi)^2}\frac{(\chi_{\mathbf{k}}^{*(1)}\chi_{\mathbf{k}_1}^{(1)})(\chi_{\mathbf{k}_1}^{*(1)}\chi_{\mathbf{k}_1+\mathbf{k}_2-\mathbf{k}}^{(1)})(\chi_{\mathbf{k}_1+\mathbf{k}_2-\mathbf{k}}^{*(1)}\chi_{\mathbf{k}_2}^{(1)})(\chi_{\mathbf{k}_2}^{*(1)}\chi_{\mathbf{k}}^{(1)})}{[E - E_1(\mathbf{k}_1)][E - E_1(\mathbf{k}_2)][E - E_1(\mathbf{k}_1 + \mathbf{k}_2 - \mathbf{k})]}, \tag{15}$$

respectively. Noting that the scalar products $(\chi^{*(1)}_{\mathbf{k}}\chi^{(1)}_{\mathbf{k}'})$ are equal to

$$(\chi^{*(1)}_{\mathbf{k}}\chi^{(1)}_{\mathbf{k}'})=\cos\left(\frac{\phi_{\mathbf{k}}-\phi_{\mathbf{k}'}}{2}\right)e^{-i[(\phi_{\mathbf{k}}-\phi_{\mathbf{k}'})/2]}, \tag{16}$$

the integration over the angles $\phi_{\mathbf{k}_1}$ and $\phi_{\mathbf{k}_2}$ in Eq. (14) can be easily performed. The main contribution to the integrals over absolute values k_1 and k_2 comes from the regions $|k_1-k_0|\ll k_0$, $|k_2-k_0|\ll k_0$. Then, using Eq. (12) and performing the integration over k_1 and k_2, we obtain the following estimate for Im $\Sigma^{(1)}$:

$$\text{Im }\Sigma^{(1)}\sim\gamma^2\frac{m}{\hbar^2}\frac{k_0^2}{|E+\Delta|}. \tag{17}$$

In contrast to Eq. (14), in the second diagram the condition that the magnitudes of $\mathbf{k}$, $\mathbf{k}_1$, and $\mathbf{k}_2$ are close to k_0 restricts the integration over angles. Indeed, consider the last energy denominator in Eq. (15). One can check that the condition

$$|\mathbf{k}_1+\mathbf{k}_2-\mathbf{k}|-k_0\sim\sqrt{m|E+\Delta|/\hbar^2} \tag{18}$$

confines one of the integration angles within the range $\phi\sim\sqrt{m|E+\Delta|}/(\hbar k_0)$. Then the estimate for Im $\Sigma^{(2)}$ yields

$$\text{Im }\Sigma^{(2)}\sim\gamma^2\left(\frac{mk_0}{\hbar^2|E+\Delta|}\right)^{3/2}. \tag{19}$$

Thus we obtain the following estimate for the ratio of diagrams (a) and (b)

$$\frac{\text{Im }\Sigma^{(2)}}{\text{Im }\Sigma^{(1)}}\sim\sqrt{m|E+\Delta|}/(\hbar k_0). \tag{20}$$

In the region of broadening, $|E+\Delta|\sim E_{1D}$, this ratio is of the order of $\kappa^{1/3}\ll 1$.

Once the diagrams with self-intersections can be neglected, the summation of the remaining series is straightforward, and yields the following equation for the self-energy:

$$\text{Im }\Sigma_{\mathbf{k}}(E)=\gamma\ \text{Im}\int\frac{d^2\mathbf{k}_1}{(2\pi)^2}\frac{|(\chi^{*(1)}_{\mathbf{k}}\chi^{(1)}_{\mathbf{k}_1})|^2}{E-E_1(\mathbf{k}_1)-\Sigma_{\mathbf{k}_1}(E)}. \tag{21}$$

Noting that Im $\Sigma_{\mathbf{k}}(E)$ does not depend on $\mathbf{k}$ (the explicit dependence on $\phi_{\mathbf{k}}$ disappears after the angular integration), and using the expression (12) for $E_1(\mathbf{k}_1)$, we obtain

$$\text{Im }\Sigma=\frac{E_{1D}}{2^{4/3}}f\left(\frac{2^{4/3}\varepsilon}{E_{1D}}\right), \tag{22}$$

where the energy ε is defined as

$$\varepsilon=E+\Delta-\text{Re }\Sigma, \tag{23}$$

and the dimensionless function $f(x)$ satisfies the algebraic equation

$$f(x)=\sqrt{\frac{x+\sqrt{f(x)^2+x^2}}{f(x)^2+x^2}}. \tag{24}$$

The function $f(x)$ is shown in Fig. 2. It turns to zero at $x=-2^{-1/3}$. In the vicinity of $x=-2^{-1/3}$, it exhibits a square-root behavior $f(x)\simeq 2^{5/6}3^{1/2}\sqrt{x+2^{-1/3}}/5^{1/2}$, which is usual for the coherent potential approximation. Using Eq. (21), the density of states (13) can be expressed through the function $f(x)$ as follows:

$$\rho(\varepsilon)=\frac{1}{\pi\gamma}\text{Im }\Sigma=\frac{m}{2\pi\hbar^2}\left(\frac{4}{\kappa}\right)^{1/3}f\left(\frac{2^{4/3}\varepsilon}{E_{1D}}\right). \tag{25}$$

Clearly, the vanishing of the DOS at $\varepsilon=-2^{-5/3}E_{1D}$ is the consequence of neglecting the diagrams with self-intersections. Taking these diagrams into account leads to the smearing of this singularity and the formation of the tail of the DOS. The fact that intersecting diagrams are relatively small indicates that the characteristic energy for this smearing should be much smaller than E_{1D}. Indeed, below we demonstrate, using the instanton approach, that the DOS in the tail has the form

$$\rho(\varepsilon)\propto\exp\left(-\frac{\pi|\varepsilon|}{E_{2D}\ln(\Delta/|\varepsilon|)}\right). \tag{26}$$

It is seen from Eq. (26) that the rate of the decay of the DOS in the tail is $E_{2D}\ln(\Delta/E_{2D})\ll E_{1D}$. Note that, at $|\varepsilon|\sim\Delta$, Eq. (26) matches the result (1) for the zero SO coupling. This conclusion could be anticipated since at energies $|\varepsilon|\gg\Delta$ the density of states does not depend on the SO coupling, and Eq. (1) applies.

Within the instanton approach the density of states is given by

$$\rho(E)\propto\exp\left(-\frac{1}{2\gamma}\int d^2\mathbf{r}|\Phi(\mathbf{r})|^4\right), \tag{27}$$

where the function $\Phi(\mathbf{r})$ is the solution of the nonlinear equation

$$\hat{H}\Phi(\mathbf{r})-|\Phi(\mathbf{r})|^2\Phi(\mathbf{r})=E\Phi(\mathbf{r}). \tag{28}$$

When the energy E is close to $-\Delta$, the two-component wave function $\Phi(\mathbf{r})$ is modulated in space with a period $2\pi/k_0$. Then it is convenient to perform the Fourier transformation of Eq. (28). Substituting

$$\Phi(\mathbf{r})=\int d^2\mathbf{r}\ A(\mathbf{k})\chi^{(1)}_{\mathbf{k}}e^{-i\mathbf{k}\cdot\mathbf{r}}, \tag{29}$$

we obtain

$$\begin{aligned}A(\mathbf{k})[E_1(\mathbf{k})-E]=\frac{1}{(2\pi)^2}\int d^2\mathbf{r}\int\left(\prod_{i=1,2,3}d^2\mathbf{k}_iA(\mathbf{k}_i)\right)\\ \times(\chi^{*(1)}_{\mathbf{k}}\chi^{(1)}_{\mathbf{k}_1})\\ \times(\chi^{*(1)}_{\mathbf{k}_2}\chi^{(1)}_{\mathbf{k}_3})e^{i(\mathbf{k}_1-\mathbf{k}_2+\mathbf{k}_3-\mathbf{k})\cdot\mathbf{r}}.\end{aligned} \tag{30}$$

Since $A(\mathbf{k})$ depends only on the absolute value of $\mathbf{k}$, the angular integration in Eq. (30) can be easily performed. Using Eq. (16), we obtain

$$A(k)[E_1(\mathbf{k})-E]$$
$$=\pi^2\int dr\ r\int\left(\prod_{i=1,2,3}dk_i k_i A(k_i)\right)$$
$$\times[J_0(kr)J_0(k_1r)+J_1(kr)J_1(k_1r)]$$
$$\times[J_0(k_2r)J_0(k_3r)+J_1(k_2r)J_1(k_3r)], \tag{31}$$

where $J_0(x)$ and $J_1(x)$ are the Bessel functions of the zeroth and first orders, respectively. Now we make use of the fact that for $E\approx-\Delta$ the typical range of the change of each k is $|k-k_0|\sim k_\varepsilon=\sqrt{m(E+\Delta)/\hbar^2}$. If we replace k, k_1, k_2, and k_3 in the arguments of Bessel functions by k_0, then the product of Bessel functions will fall off as r^{-2}, and the integral over r would diverge logarithmically at $r\to\infty$. Cutting this divergence at $r\sim k_\varepsilon^{-1}$ we obtain

$$A(k)\left(\frac{\hbar^2}{2m}(k-k_0)^2-\varepsilon\right)=4k_0\ln\frac{k_0}{k_\varepsilon}\left(\int_0^\infty dk' A(k')\right)^3. \tag{32}$$

The obvious solution of this equation is

$$A(k)=\frac{C}{\frac{\hbar^2}{2m}(k-k_0)^2+|\varepsilon|}. \tag{33}$$

Substituting Eq. (33) into Eq. (32), we find the value of the constant C,

$$C=\frac{1}{2\pi^{3/2}}k_0^{-1/2}\left(\frac{2m}{|\varepsilon|\hbar^2}\right)^{-3/4}\ln^{-1/2}(k_0/k_\varepsilon). \tag{34}$$

Performing the inverse Fourier transformation, we obtain the solution of the instanton equation in the coordinate space, which is valid for $r\lesssim k_\varepsilon^{-1}$:

$$\Phi(r)=2\pi^2 C k_0\left(\frac{m}{\hbar^2|\varepsilon|}\right)^{1/2}\begin{pmatrix}J_1(k_0r)\\-J_0(k_0r)\end{pmatrix}. \tag{35}$$

Finally, upon substituting Eq. (35) into Eq. (27) we arrive at Eq. (26).

In conclusion, we have calculated the DOS for 2D electrons in the Gaussian random potential in the limit of a strong spin-orbit coupling. The summation of the diagram series became possible due to the fact that in the absence of disorder the energy spectrum has a minimum at some finite $k=k_0$. This causes he magnitude of smearing of the DOS to increase with increasing the strength of the SO coupling.

The physical origin of the SO-induced enhancement of the width is the following. It is well known that without SO coupling an arbitrary weak attractive potential creates a bound state which in the 2D case is exponentially shallow.[11] In the presence of the SO coupling the same model quantum-mechanical problem can be easily solved. The solution indicates that the bound state is always present for an arbitrary weak attraction and, moreover, that its binding energy is much greater (quadratic instead of exponential with respect to the attraction strength) than without SO coupling. It is obvious that as the strength of the attractive potential increases, so that the binding energy grows, the difference between the two cases gradually vanishes.

Note that the depth of the minimum in the energy spectrum decreases in the presence of a magnetic field, and disappears completely when the Zeeman splitting exceeds 2Δ. This suggests that the tail of the DOS is very sensitive to a weak magnetic field. The latter property (disappearing of a peak in DOS at small fields) can be used as an experimental test of the theory in optical absorption.

The applicability of the theory developed requires the SO-induced energy scale Δ to be larger than the inverse relaxation time E_{2D} in the absence of the SO coupling. This condition seems to be met in high-mobility silicon metal-oxide semiconductor field-effect transistors.[12,13] According to Ref. 13, the coupling constant α in this structures is $\sim 2\times10^{-6}$ meV cm, which corresponds to $\Delta\sim1$ K. However, in the experimentally interesting situation where the metal-insulator transition occurs (see, e.g., recent references[14]), the Fermi energy lies much higher than Δ.

[1] D. J. Thouless and M. E. Elzain, J. Phys. C **11**, 3425 (1978).
[2] E. Brézin and G. Parisi, J. Phys. C **13**, L307 (1980).
[3] B. I. Halperin and M. Lax, Phys. Rev. **148**, 722 (1966).
[4] J. Zittartz and J. S. Langer, Phys. Rev. **148**, 741 (1966).
[5] B. I. Shklovskii and A. L. Efros, *Electronic Properties of Doped Semiconductors* (Springer, Berlin, 1984).
[6] I. M. Lifshitz, S. A. Gredeskul, and L. A. Pastur, *Introduction to the Theory of Disordered Systems* (Wiley, New York, 1988).
[7] G. Dresselhaus, Phys. Rev. **100**, 580 (1955).
[8] P. D. Dresselhaus *et al.*, Phys. Rev. Lett. **68**, 106 (1992).
[9] Yu. A. Bychkov and E. I. Rashba, Pis'ma Zh. Éksp. Teor. Fiz. **39** 64 (1984) [JETP Lett. **39**, 78 (1984)].
[10] A. L. Efros and M. E. Raikh, in *Optical Properties of Mixed Crystals*, edited by R. J. Elliot and I. P. Ipatova (Elsevier, Amsterdam, 1998), p. 133.
[11] L. D. Landau and E. M. Lifshitz, *Quantum Mechanics* (Pergamon, New York, 1977).
[12] V. M. Pudalov *et al.*, Pis'ma Zh. Éksp. Teor. Fiz. **65**, 887 (1997) [JETP Lett. **65**, 932 (1997)].
[13] V. M. Pudalov, cond-mat/9707076; Pis'ma Zh. Eksp. Teor. Fiz. **66**, 168 (1997) [JETP. Lett. **66**, 175 (1997)].
[14] S. V. Kravchenko *et al.*, Phys. Rev. Lett. **77**, 4938 (1996); D. Popović, A. B. Fowler, and S. Washburn, *ibid.* **79**, 1543 (1997); D. Simonian *et al.*, *ibid.* **79**, 2304 (1997).